Decay-rate dependence of anhysteretic remanence: Fundamental origin and paleomagnetic applications

Yongjae Yu[1] and David J. Dunlop[1]

Geophysics, Department of Physics, University of Toronto, Mississauga, Ontario, Canada

Received 16 May 2003; revised 28 August 2003; accepted 17 September 2003; published 3 December 2003.

[1] We have measured the intensity of anhysteretic remanent magnetization (ARM) as a function of alternating field (AF) decay rate. For synthetic and natural single-domain (SD) and pseudo-single-domain (PSD) magnetites, ARM intensity increases as decay rate decreases. Multidomain (MD) magnetites have the opposite response, ARM increasing as the decay rate increases. These are identical to the SD/PSD and MD dependences of thermoremanent magnetization on cooling rate. For all grain sizes and domain structures, ARM intensity increases as the AF decay rate used to achieve an initial demagnetized state decreases. Decay-rate differences in ARM intensity are a property of low- and medium-coercivity grains, as shown by annealing and by stepwise AF demagnetizing samples. We interpret the SD results to mean that increased AF exposure time permits a closer approach to equilibrium magnetization. An approximate thermal activation theory based on *Néel* [1949] and an exact theory by *Egli and Lowrie* [2002] predict 6−11% increases in ARM for an order of magnitude decrease in decay rate, in reasonable accord with the observed 12% increase for 0.065 μm SD grains. For MD grains, we hypothesize that increased exposure time (slower decay) permits more efficient self-demagnetization, reducing ARM. Low-coercivity grains experience the largest self-demagnetizing fields and therefore have the largest decay-rate response. Initial-state decay-rate response is attributed to longer exposure times leaving domain walls more strongly pinned in deeper potential wells (the net self-demagnetizing field is zero in the demagnetized state). Acquisition decay-rate, annealing, and initial-state responses of PSD grains are a blend of SD and MD responses. Because ARM is the most frequently used normalizer in relative paleointensity determination, it is important either to use a standard decay rate or else to remove the decay-rate dependence by demagnetizing the ARM to ∼30% of its initial value ($ARM_{0.3}$). A standard demagnetization level for the normalizing ARM is particularly important when comparing paleointensity records from different laboratories. *INDEX TERMS:* 1512 Geomagnetism and Paleomagnetism: Environmental magnetism; 1521 Geomagnetism and Paleomagnetism: Paleointensity; 1527 Geomagnetism and Paleomagnetism: Paleomagnetism applied to geologic processes; 1540 Geomagnetism and Paleomagnetism: Rock and mineral magnetism; 1594 Geomagnetism and Paleomagnetism: Instruments and techniques; *KEYWORDS:* anhysteretic remanence (ARM), decay rate, relative paleointensity, alternating field (AF)

Citation: Yu, Y., and D. J. Dunlop, Decay-rate dependence of anhysteretic remanence: Fundamental origin and paleomagnetic applications, *J. Geophys. Res.*, *108*(B12), 2550, doi:10.1029/2003JB002589, 2003.

1. Introduction

[2] Anhysteretic remanent magnetization (ARM) is produced by the combination of a slowly decaying alternating field (AF) $\widetilde{H}$ and a steady unidirectional field $\boldsymbol{H}$. As a quick and non-destructive technique, ARM has been widely used in environmental magnetism and paleomagnetism [*Tauxe*, 1993; *Verosub and Roberts*, 1995; *Dunlop and Özdemir*, 1997]. In particular, the ratio of ARM to magnetic susceptibility [*Levi and Banerjee*, 1976; *Banerjee et al.*, 1981] or ARM to saturation isothermal remanent magnetization (SIRM) [*Doh et al.*, 1988; *Stoner et al.*, 1995] is a commonly used proxy for grain size. In rock magnetism, the similarity of AF demagnetization spectra of ARM and thermoremanent magnetization (TRM) has provided a rationale for the use of ARM instead of TRM in the Lowrie-Fuller test [*Lowrie and Fuller*, 1971; *Johnson et al.*, 1975].

[3] ARM is routinely used in sediments as a normalizing remanence (NRM/ARM) in relative geomagnetic field intensity determination [*Tauxe*, 1993]. ARM has also been adopted in the pseudo-Thellier paleointensity method [*Tauxe et al.*, 1995]. It is common practice to stack relative paleointensity data obtained from different studies [e.g., *Guyodo*

[1]Currently at Geosciences Research Division, Scripps Institution of Oceanography, La Jolla, California, USA.

0148-0227/03/2003JB002589$09.00

Table 1. Synthetic Samples[a]

Sample	Powder	*d*, μm	*n*	M_{rs}/M_s	H_{cr}/H_c	MDF, mT
1	4000	0.065	884	0.41	1.36	28
2	5099	0.21	1300	0.23	1.97	24
3	112978	0.44	1022	0.12	2.92	30
4	M	0.24	532	0.37	1.94	28
5	5000	0.34	1262	0.36	1.57	34
6	3006	1.06	1471	0.29	1.78	33
7	112982	16.9	1618	0.06	6.47	10
8	041183	18.3	870	0.07	5.14	10

[a]Powders 4000, 112978, 5000, 3006, 112982, and 041183 are from the Wright Company; powders 5099 and M are the products of Pfizer and Mapico Companies. The estimated mean grain size *d* was determined using the scanning electron microscope (SEM). *n* is the number of grains counted under the SEM. MDF is the median destructive field determined from AF demagnetization of ARM; hysteresis parameters were measured from 6 or more chips of sister specimens; values of saturation magnetization (M_s), saturation remanence (M_{rs}), and coercive force (H_c) were determined from hysteresis loops; values of remanence coercivity (H_{cr}) were obtained from backfield measurements.

and Valet, 1999]. If the intensity of ARM depends on the experimental conditions used in producing the ARM, any subsequent stacking or comparison would be compromised.

[4] Several factors influence the intensity of ARM. First, ARM has a grain size dependence [*Levi and Merrill*, 1976; *Dunlop and Argyle*, 1997], being more intense in small grains than in large grains, as is also true for TRM. Second, for a fixed grain size of magnetite, ARM depends on magnetic concentration [*Sugiura*, 1979; *King et al.*, 1983; *Yamazaki and Ioka*, 1997]. In general, higher magnetic concentration causes stronger interactions among magnetic grains, lowering ARM intensity. Third, ARM intensity is dependent on peak AF intensity. Some instruments have peak AFs up to 100 mT while others have a limit of 200 mT. In this study, we examine a fourth factor, the dependence of ARM on the decay rate of the AF.

2. Samples and Instruments

[5] Eight synthetic samples were prepared using commercial magnetite powders whose mean grain sizes range from single domain (SD, 0.065 μm) to small multidomain (MD, 18.3 μm) [*Yu et al.*, 2002]. Grain sizes were determined using a Hitachi S-4500 scanning electron microscope (SEM). To reduce the uncertainty, ~1000 grains were typically measured from at least six SEM photos per powder. Synthetic samples are ~0.5% by volume dispersions of magnetite in a matrix of CaF_2. Cylindrical pellets 8.8 mm in diameter and 8.6 mm in height were pressed and then tightly wrapped with quartz wool inside quartz capsules. The capsules were sealed under vacuum and annealed for 3 hours at 700°C to stabilize the magnetic properties. Detailed magnetic properties of these synthetic magnetites have been published elsewhere (*Yu et al.* [2002], Tables 1 and 2). Only a brief summary of rock magnetic parameters is given in Table 1.

[6] Twenty-six natural samples were also studied: two andesites [*Yu*, 1998], fourteen gabbros [*Yu and Dunlop*, 2001, 2002], three granites [*Dunlop*, 1984; *Dunlop et al.*, 1984], and seven freeze-dried lake sediments [*Brachfeld and Banerjee*, 2000]. The magnetic and paleomagnetic properties of the natural samples are well documented in these papers. A summary appears in Table 2. The samples are cylindrical, 2.3 cm in diameter and 2.0 cm long. They were chosen from a large collection of several hundred cores on the basis of their low magnetic anisotropy, their reproducible ARM intensities, and minimal viscous magnetic changes [*Yu et al.*, 2002]. The gabbros and lake sediments had given reliable paleointensities by the Thellier and pseudo-Thellier methods, respectively.

[7] To test the decay-rate dependence of ARM, we used a Molspin AF demagnetizer that generates peak AFs up to 100 mT at 180 Hz. Four different decay rates are available, denoted by A (4 μT/cycle or 0.72 mT/s), B (9 μT/cycle or 1.62 mT/s), C (19 μT/cycle or 3.42 mT/s), and D (35 μT/cycle or 6.30 mT/s).

[8] Sample were AF demagnetized to 100 mT before each ARM acquisition experiment. ARM was produced in a peak AF of 100 mT with $\boldsymbol{H}$ = 100 μT. Decay rates during initial AF demagnetization and later ARM acquisition will be denoted by subscripts and superscripts, respectively. For example, ARM_D^A indicates that the sample was initially AF demagnetized at decay rate D while the subsequent ARM was acquired at decay rate A. All the comparisons of intensity are normalized to ARM_D^D, which was the quickest to produce.

3. Dependence of Anhysteretic Remanent Magnetization (ARM) Intensity on Alternate Field (AF) Decay Rate

[9] In the experiments described in this section, decay rate D (6.3 mT/s) was used for all initial AF demagnetizations and the decay rate was varied for ARM acquisition. In Figure 1, ARM intensity is plotted as a function of decay rate, on both logarithmic (Figure 1a, 1b) and linear (Figure 1c, 1d) scales. For synthetic SD (0.065 μm) magnetite, ARM intensity decreases 12.5% as the decay rate increases from 0.72 mT/s to 6.3 mT/s (Figure 1a, 1c). A similar but less pronounced trend was observed for synthetic pseudo-single-domain (PSD) magnetites (0.24 and 1.06 μm). Synthetic MD magnetite shows the opposite trend, however. ARM intensity increases ~10% as the decay rate increases by an order of magnitude. The amount of increase or decrease is less for unannealed grains than for annealed grains of the same size. Internal stress apparently reduces the decay-rate dependence of ARM (Figure 1a, 1c).

[10] Similar behavior was observed for natural samples (Figure 1b, 1d). Samples C6C1 (Cordova Gabbro, ON, Canada) and 456 B (Lake sediments, Lake Pepin, MN, USA), An 3 (An-ei Andesite, Mt. Sakurajima, Japan), and

Table 2. Natural Samples[a]

Samples	T_{UB}, °C	MDF, mT	M_{rs}/M_s	H_{cr}/H_c
An-ei basalts	580	30	0.28	2.11
Kometsuka red-scoria	500	48	0.39	1.65
Tudor Gabbro	580	37	0.34	1.70
Cordova Gabbro	580	40	0.32	1.82
Burchell Lake Granite	580	15	0.04	4.72
Shelley Lake Granite	580	13	0.04	4.39
Lake Pepin sediments	n.a.	32	0.23	2.09

[a]T_{UB} is the maximum unblocking temperature from the thermal demagnetization of sister specimens; n.a. is not available. MDF is the median destructive field determined from AF demagnetization of ARM; hysteresis parameters were measured from 6 or more chips of sister specimens; values of saturation magnetization (M_s), saturation remanence (M_{rs}), and coercive force (H_c) were determined from hysteresis loops; values of remanence coercivity (H_{cr}) were obtained from backfield measurements.

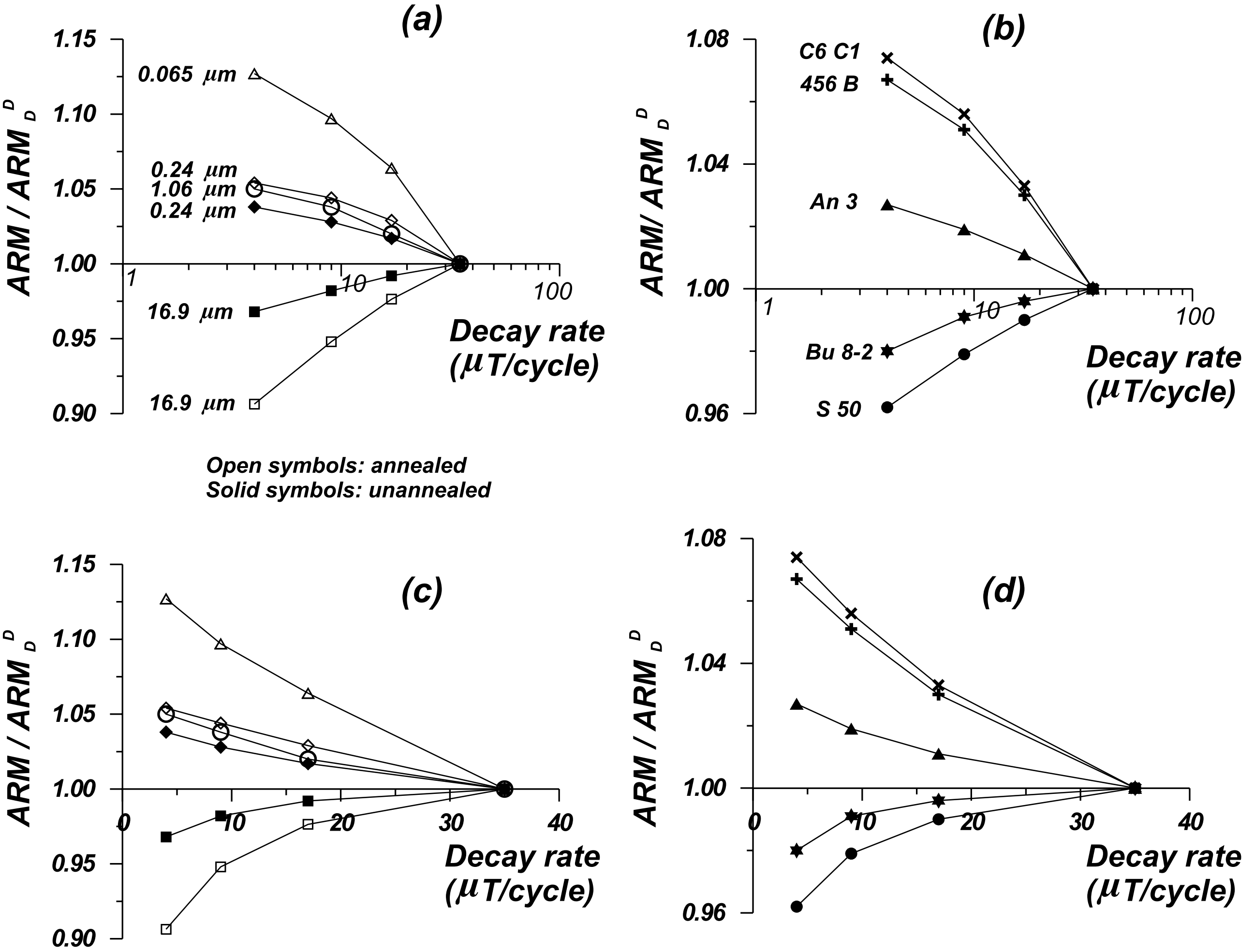

Figure 1. Acquisition decay-rate dependence of ARM for (a, c) synthetic and (b, d) natural samples. Initially AF demagnetization was at decay rate D (35 µT/cycle or 6.3 mT/s). Subsequent ARM acquisition used decay rates from A (4 µT/cycle or 0.72 mT/s) to D.

Bu 8-2 (Burchell Lake Granite, ON, Canada) and S 50 (Shelley Lake Granite, ON, Canada) mimic trends of very fine PSD, larger PSD, and MD grains, respectively. Their magnetic properties (Table 2) are in accord with these implied domain states.

[11] For synthetic SD and PSD magnetite and natural samples containing PSD magnetite, the rate of ARM decrease (on a logarithmic decay-rate scale) is larger at faster decay rates (C, D) than that at slower decay rates (A, B) (Figure 1a, 1b). For synthetic MD samples and granites, the rate of ARM increase is nearly linear, although slightly larger at slower decay rates (A, B) than at faster decay rates (C, D).

4. Dependence of ARM Intensity on AF Demagnetization Decay Rate

[12] In section 3, ARM was produced from a standard initial demagnetized state that used an AF decay rate of 6.3 mT/s. In this section, we vary the decay rate for AF demagnetization as well as the AF decay rate used for ARM acquisition. For example, ARM_B^C was initially AF demagnetized at decay rate B (1.62 mT/s) and then ARM was produced using AF decay rate C (3.42 mT/s). Since we tested four different decay rates for both AF demagnetization and ARM acquisition, 16 different types of ARMs had to be produced and measured for each sample.

[13] In order to test the repeatability of the measurements, each of the 16 types of ARM was replicated six times. Plotted values are averages of these six measurements. Dispersion within each set of 6 measurements was typically <1%. Individual measurements were in the range 30–1500 mA/m, compared to the Molspin instrumental noise level of 0.1–1 mA/m.

[14] Intensity differences among ARMs of different types are small but very consistent. Two typical examples are illustrated in Figure 2. For a fixed decay rate during ARM acquisition, we found always $ARM_A > ARM_B > ARM_C > ARM_D$, regardless of grain size or rock type. Apart from this offset in intensities, each decay rate during AF demagnetization yielded the same dependence of ARM intensity on acquisition decay rate.

5. AF Demagnetization of ARMs With Different Acquisition Decay Rates

[15] We next measured the stepwise AF demagnetization of ARMs of selected samples. AF demagnetization

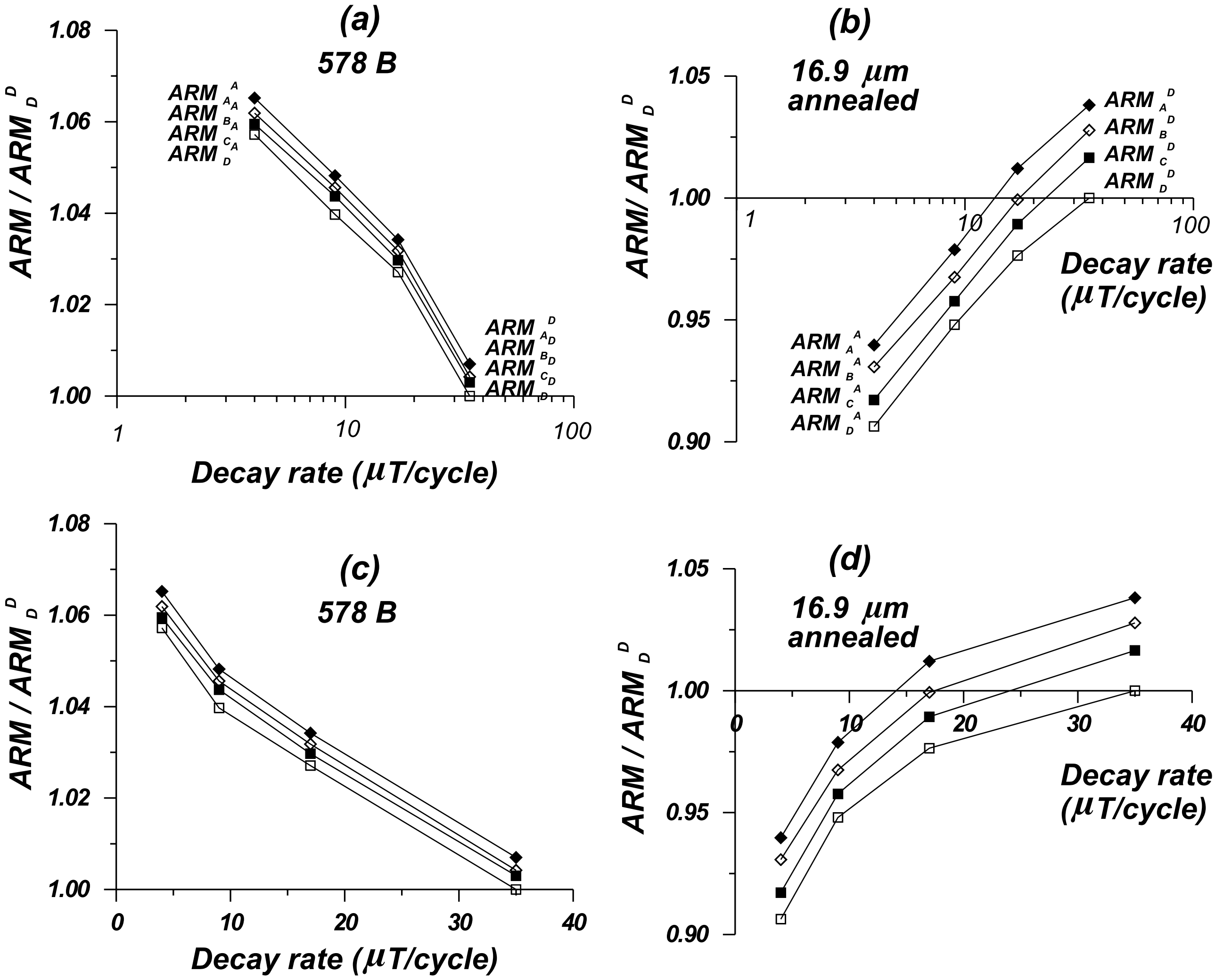

Figure 2. Initial-state decay-rate dependence of ARM for (a, c) 578 B (lake sediments, Lake Pepin, MN, USA) and (b, d) synthetic MD magnetite (16.9 μm). Decay rates used during initial AF demagnetization and later ARM acquisition are denoted by subscripts and superscripts, respectively. A, B, C, D: 4, 9, 19, 35 μT/cycle.

curves of ARM_A^A, ARM_A^B, ARM_A^D, ARM_D^A, and ARM_D^D are compared in Figure 3a for lake sediment 578 B and in Figure 3b for annealed MD (16.9 μm) magnetite. All AF demagnetization curves converge when the ARM is reduced to ~30% of its initial value, which occurs around 40 mT for 578 B and around 10 mT for the 16.9 μm magnetite. Thus ARM intensity differences due to varying decay rates are confined to low (Figure 3b) to intermediate (Figure 3a) coercivities. AF demagnetization curves of ARM_Bs and ARM_Cs (not shown) fall within the envelope between ARM_A^A and ARM_D^D.

6. Discussion and Interpretation

6.1. Comparison of Rate Dependences of Thermoremanent Magnetization (TRM) and ARM

[16] Theoretically the TRM intensity of SD grains should decrease as the cooling rate increases [*Néel*, 1955; *Pullaiah et al.*, 1975; *York*, 1978; *Halgedahl et al.*, 1980; *Dodson and McClelland-Brown*, 1980; *Walton*, 1980; *Walton and Williams*, 1988]. This prediction has been experimentally confirmed by studies on archeological baked clay [*Fox and Aitken*, 1980] and on SD hematite [*Papusoi*, 1972a]. The same trend was confirmed for PSD size grains in baked clays, potsherds, and volcanic rocks [*Yang et al.*, 1993; *Biquand*, 1994; *Chauvin et al.*, 2000]. However, exactly the opposite trend was observed for MD magnetite [*Papusoi*, 1972b] (see also *McClelland-Brown* [1984]; *Perrin* [1998]) and remains unexplained.

[17] As with the cooling rate dependence of TRM, we anticipate that the ARM intensity in SD grains should increase as the decay rate decreases. In both cases a longer exposure time at temperature T or AF $\widetilde{H}$ allows a closer approach to equilibrium magnetization. Synthetic SD and PSD magnetites and natural samples containing PSD magnetite obeyed this prediction, but grains of MD size had the opposite trend, showing an increase of ARM intensity as decay rate increases (Figure 1). The decay rate response of ARM thus matches the cooling rate

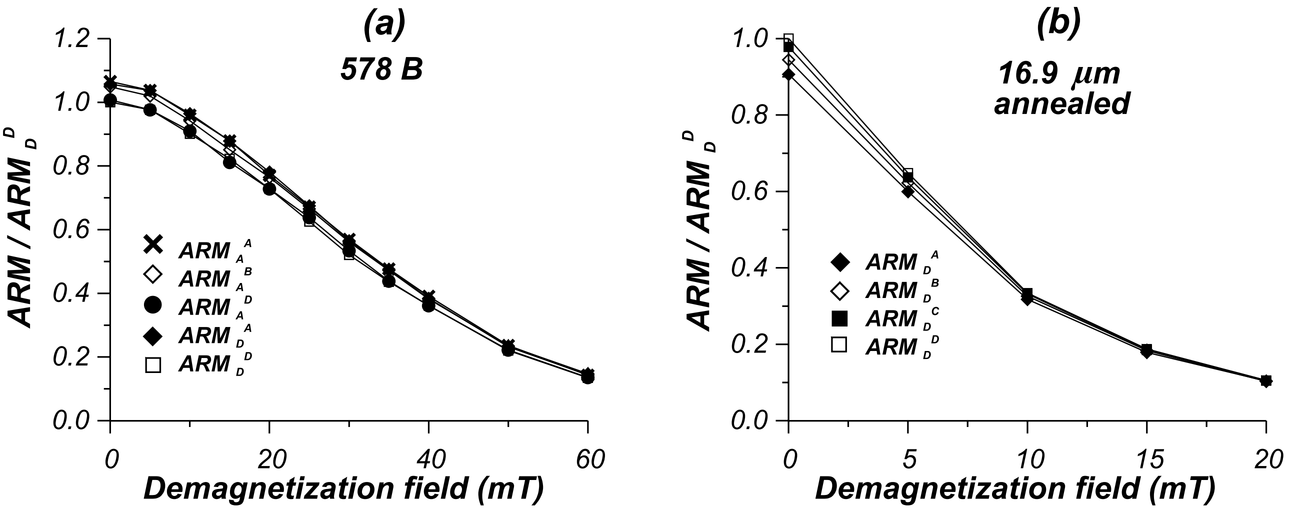

Figure 3. AF demagnetization of ARMs for (a) 578 B, (b) 16.9 μm magnetite. Decay rates during initial AF demagnetization and later ARM acquisition are denoted by subscripts and superscripts, respectively. Demagnetization curves converge when ARM is reduced to ~30% of initial intensity, which requires AFs of ~40 mT for (a) and ~10 mT for (b).

response of TRM for MD grains, as well as for SD/PSD grains.

6.2. Observational Constraints and Explanation of Pseudo-Single-Domain (PSD) Trends

[18] Modeling of the origin of decay-rate effects is constrained by the following observations.

[19] 1. The dependence of ARM intensity on the decay rate of the AF used to produce it is negative for SD and PSD-size magnetites (i.e., ARM decreases as decay rate increases) but there is a positive dependence for MD magnetites (Figure 1).

[20] 2. The dependence of ARM intensity on the decay rate of the AF used to produce an initial demagnetized state is negative for magnetites of all sizes (Figure 2).

[21] 3. The magnitude of dependence 1 varies with grain size and domain structure. SD and MD grains have larger decay-rate dependences than PSD grains (Figure 1).

[22] 4. The magnitude of dependence 1 varies with annealing. Annealed PSD and MD magnetites have larger dependences than unannealed grains of the same size and origin (Figure 1). Internal stress reduces the dependence of ARM intensity on AF decay-rate.

[23] 5. ARM differences are confined to low- and medium-coercivity fractions and are eliminated by AF demagnetization to ~30% of the initial ARM intensity (Figure 3). This is true for all sizes/domain states.

[24] If PSD behavior is due to a simple mixture of SD and MD sources, as separate grains or as independent regions within grains [*Dunlop and Özdemir*, 1997, Chaps. 5, 12; *Dunlop*, 2002], the observations for PSD samples can be explained by superposition. The PSD decay-rate dependence of ARM is the sum of a negative SD dependence and a positive MD dependence. For small PSD grains like the 0.24 μm and 1.06 μm ones in Figure 1, the SD contribution is larger than the MD and the net dependence is negative. The effect of annealing on the ARM rate dependence of the 0.24 μm grains is smaller than the effect of annealing on 16.9 μm MD grains because only a fraction of the ARM of the 0.24 μm grains has an MD source.

6.3. Single-Domain (SD) Theories of the Decay Rate Dependence of ARM

[25] Now we require theories to explain the differing responses of SD and MD grains. In the SD case, we follow *Néel*'s [1949, 1955] thermal activation theory, which has been successfully adapted for the effect of variable cooling rates on TRM. In a weak field $\boldsymbol{H}$ aligned with the shape anisotropy axis, the intensity M_{tr} of TRM is predicted to be

$$M_{tr} = M_{rs} \tanh[\mu_o V M_s(T_B) H / kT_B], \tag{1}$$

where M_{rs} is saturation remanence, M_s is spontaneous magnetization, V is grain volume, T_B is blocking temperature, and k is Boltzmann's constant. For blocking to occur within a time t,

$$\ln(f_o\, t) = \mu_o V M_s(T_B) H_K(T_B)/2kT_B, \tag{2}$$

where H_K is microscopic coercive force and the atomic reorganization frequency f_o is $\sim 10^{-9}$ s^{-1} [*McNab et al.*, 1968; *Moskowitz et al.*, 1997; *Egli and Lowrie*, 2002]. Combining (1) and (2),

$$M_{tr}/M_{rs} = 2\ \ln(f_o\, t) H / H_K(T_B). \tag{3}$$

[26] To model ARM, we again consider an ensemble of uniaxial SD grains of volume V and microscopic coercive force $H_{Ko} = H_K(T_o)$ with easy axes parallel to the axis of the AF $\widetilde{H}$ and the steady field $\boldsymbol{H}$. Two orientations are possible for the magnetic moment $\boldsymbol{m} = V\boldsymbol{M}_s$, parallel or antiparallel to $\boldsymbol{H}$. For either of these, the lowest-energy state has $\widetilde{H}$ in the same direction as $\boldsymbol{m}$, giving energies $E = -\mu_o V M_s(\widetilde{H} \pm H)$. Because of the symmetry of the AF, each positive value of $\widetilde{H}$ has a matching negative $\widetilde{H}$ of equal magnitude.

Table 3. Predicted AF Decay Rate Dependences of ARM Intensity for SD Grains

α, μT/cycle	α, μT/s	t (s) from (7)	$\frac{M_{ar}(\alpha)}{M_{ar}(\alpha_0)}$ from (5)	$\frac{M_{ar}(\alpha)}{M_{ar}(\alpha_0)}$ from (8)
4	0.72	1.819	1.112	1.057
9	1.62	0.8083	1.070	1.037
19	3.42	0.3829	1.031	1.017
35	α_0 = 6.30	0.2079	1.000	1.000

[27] The equilibrium ARM is given by a Boltzmann partition between pairs of energy states with matching $\widetilde{H}$ values:

$$M_{ar}/M_{rs} = \left[\exp\left(-\mu_o VM_s\left(\widetilde{H} - H\right)/kT_o\right) - \exp\left(-\mu_o VM_s\left(\widetilde{H} + H\right)/kT_o\right)\right] / \left[\exp\left(-\mu_o VM_s\left(\widetilde{H} - H\right)/kT_o\right) + \exp\left(-\mu_o VM_s\left(\widetilde{H} + H\right)/kT_o\right)\right] = \tanh\left[\mu_o VM_s(T_o)H)/kT_o\right]. \quad (4)$$

The counterpart to equation (3) is

$$M_{ar}/M_{rs} = 2\ \ln(f_o\, t)H/H_{Ko} \quad (5)$$

According to equations (3) and (5), ARM intensity is always less than TRM intensity, since $H_K(T_B) < H_{Ko} = H_K(T_o)$.

[28] To calculate TRM or ARM intensity as a function of the rate of change of temperature T or AF $\widetilde{H}$ it is necessary to find the effective value of t that corresponds to a specified cooling or decay rate. For TRM, *Stacey and Banerjee* [1974] and *York* [1978] arrived at the approximate expression

$$t = [kT_B/\Delta E(T_B)][T_B/(-\mathrm{d}T/\mathrm{d}t)], \quad (6)$$

in which ΔE is the energy barrier over which the SD moment must be activated. $\Delta E(T_B)/kT_B$ is given explicitly by the r.h.s. of (2). In deriving (6), both authors neglected the change in ΔE over the range of T in which blocking occurs (the mean of which is T_B).

[29] Appealing to the analogy between blocking with a decaying AF and with changing temperature [*Dunlop and West*, 1969], we propose as an ARM counterpart to (6)

$$t = [kT_o/\Delta E(T_o)]\left[H_{Ko}/\left(-\mathrm{d}\tilde{H}/\mathrm{d}t\right)\right]. \quad (7)$$

Calculating t from (7) for a specified AF decay rate $\alpha = \mathrm{d}\widetilde{H}/\mathrm{d}t$ and substituting in (5) gives an approximate value for ARM.

[30] An exact treatment is given by *Egli and Lowrie* [2002], who find (their equation (42))

$$M_{ar}^3(\alpha)/M_{ar}^3(\alpha_o) = a + b\ \ln\alpha, \quad (8)$$

$$a = 1 + \ln\alpha_o/\ln\left[(0.7f_o/\alpha_o vH_{Ko})(kT_o/VM_{so})^{3/2}\right], \quad (9)$$

$$b = -\ln 10/\ln\left[(0.7f_o/\alpha_o vH_{Ko})(kT_o/VM_{so})^{3/2}\right], \quad (10)$$

α_o being a reference decay rate.

6.4. Comparison of Predicted and Measured Decay Rate Dependence

[31] We now use equations (5) and (7) to predict values of ARM intensity for our 0.065 μm SD magnetite sample. The t values calculated from (7) for our range of α values (0.72–6.3 mT/s) turn out to be 0.2–1.8 secs. Thus it is reasonable to use a trial value t = 1 s along with $f_o = 1.3 \times 10^9\ s^{-1}$ [*Egli and Lowrie*, 2002], giving $\Delta E(T_o)/kT_o = \ln(f_o t) = 21.0$. For 0.065 μm grains, near the maximum size for SD behavior, the difference H_q between the microscopic coercive force in the absence of thermal fluctuations and the switching field observed in AF demagnetization is only ~1 mT (estimated from *Egli and Lowrie* [2002, Figure 10]). Thus we used H_{Ko} = 27.5 mT, the median demagnetizing field of ARM for this sample [*Yu et al.*, 2003, Figure 7]. These values when substituted in (7) along with our experimental values of α yield the t values in Table 3.

[32] Next $\ln(f_o t)$ was recomputed with the exact t values and substituted in equation (5) to find M_{ar}/M_{rs} for each value of α. The results appear in Table 3, normalized to ARM intensity for decay rate D (α_o = 6.30 mT/s). As t increases from 0.208 s to 1.82 s (decay rate decreasing by one order of magnitude), ARM intensity is predicted to increase by 11%. The observed increase is 12.5% (Figures 1 and 4).

[33] Finally we predicted absolute ARM intensities from *Egli and Lowrie*'s [2002] exact theory. With the same values of f_o, H_{Ko} and α_o as before and an average grain moment $VM_{so} = 1.30 \times 10^{-16}$ A m^2, (9) and (10) give a = 1.154 and b = −0.1924. Computing $M_{ar}^3(\alpha)/M_{ar}^3(\alpha_o)$ by substituting in (8), we arrived at the $M_{ar}(\alpha)/M_{ar}(\alpha_o)$ values in Table 3,

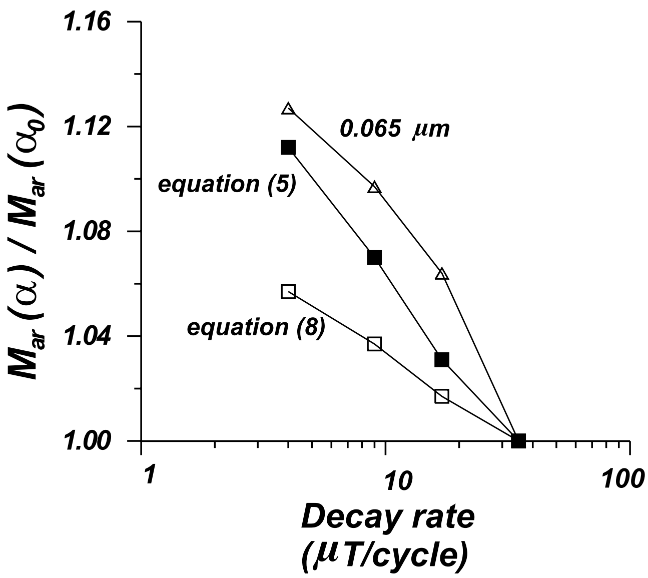

Figure 4. A comparison of observed and predicted dependences of ARM intensity on the AF decay rate in ARM acquisition for the SD (0.065 μm) sample. The approximate theory uses equations (5) and (7) of the text. The exact theory uses the results of *Egli and Lowrie* [2002] (equations (8)–(10) of the text).

which increase by about 6% as α decreases from 6.30 to 0.72 mT/s. This is about one-half the observed rate.

[34] Both the exact and approximate theories predict that for SD grains, ARM intensity increases as exposure time to $\widetilde{H}$ increases, i.e., as decay rate α decreases. An increase in ARM is logical because a longer time allows a closer approach to equilibrium alignment of SD moments, analogous to the cooling-rate dependence of TRM. However, both theories predict ARM increases that are nearly linear with log α, whereas we observe non-linear changes for the 0.065 μm and other samples.

6.5. Multidomain (MD) Model of ARM Acquisition Decay Rate Dependence

[35] In the case of MD grains, we will not attempt a numerical theory. Rather we rely on our observations to give insight into the microscopic situation. For simplicity, we ignore domain nucleation, which would produce wholesale reorganization of all walls. With a fixed population of domain walls, magnetization changes when one or more walls move between pinning sites. Pinning strength is expressed by the microcoercivity distribution. Walls move under the combined influence of the AF $\widetilde{H}$, which may lead to a higher or a lower net magnetization M, and the self-demagnetizing field H_d, which always favors a lower M. The steady field $\boldsymbol{H}$ provides a bias.

[36] In an SD grain, H_d produces a shape anisotropy barrier between states but cannot change the magnitude of M because all states have the same moment VM_s. In an MD grain with a wide range of states, H_d severely limits M. As the AF ramps down from large fields, the entire population of walls in a grain is at first mobilized. Each wall blocks as $\widetilde{H}$ drops below its microcoercivity H_c (determined by the local potential well around a dislocation or other pin) but blocking is conditional. Later movements of other walls may make $H_d > H_c$ locally and unpin the wall.

[37] Experimentally, the correlation between the decay rate used to reach a demagnetized initial state and ARM intensity produced in a later experiment is negative for both SD and MD grains (Figure 2), while the correlation between decay rate in the ARM experiment and resulting ARM intensity is negative for SD grains but positive for MD grains (Figures 1 and 4). The initial-state decay-rate correlation is a universal effect, independent of self-demagnetization. The ARM decay-rate correlation, on the other hand, must have a different cause, which in MD grains probably involves self-demagnetization. Another key factor in the ARM decay-rate effect must be microcoercivity. Decay-rate differences in ARM are larger when lower-H_c fractions are isolated, either by AF demagnetization (Figure 3) or by annealing out internal stress (Figure 1). Tightly pinned walls do not display an ARM rate dependence.

[38] Thus we can begin our theorizing at a point when the first 30% or so of the ARM, carried by the most strongly pinned walls, has been locked in. These walls are the least likely to be unpinned by later movements of the soft walls, which will continue to oscillate as $\widetilde{H}$ decays. Why should the softer walls reach a state of lower M for a slower decay rate, i.e., a longer exposure to the AF? The answer is likely that the demagnetizing field H_d due to pinned walls of higher H_c has a longer time to act. As more of the ARM is blocked, H_d grows. The result is that the time/rate effect on intensity will be largest for the last walls blocked, which will also be the first to be AF demagnetized. This is what we observe (Figure 3). This model could be tested by measuring the rate effect on partial ARMs in different coercivity ranges. Note that the same model accounts for the MD cooling-rate dependence of TRM [*Papusoi*, 1972b].

6.6. Models of ARM Initial State Decay Rate Dependence

[39] The origin of the initial-state decay-rate effect is less obvious. Traditionally a dependence of magnetic properties on prior magnetic history has been considered a property of MD grains, PSD and SD grains showing reduced effects or none at all [*Shcherbakova et al.*, 2000]. It is true that the initial-state rate dependence in Figure 2 is stronger for the 16.9 μm MD sample ($\sim$3.5% decrease between ARM_A and ARM_D) but the decrease for fine PSD sample 578 B ($\sim$1%) is still consistent and readily measurable. In the MD case, it seems that exposure to AF demagnetization for a longer time leaves the softer domain walls in somewhat deeper potential wells with higher H_c, thus rendering them less susceptible to later self-demagnetizing fields during the ARM acquisition process. The self-demagnetization effect is still dominant compared to the proposed enhanced wall pinning. The direct ARM decay-rate dependence in Figure 2b is about +10% compared to the initial-state rate dependence of about -3.5%.

[40] The only reported state dependence of SD/PSD magnetic properties is the contrast between TRM and ARM intensities for magnetites $\sim$0.07–0.5 μm in size, just above the SD critical size [*Dunlop and Argyle*, 1997]. Theoretically vortex structures should make their first appearance in this range and one can speculate that alternating fields are responsible for inducing such states and lowering ARM intensities. One could speculate further that longer exposure to AF demagnetization might produce a larger proportion of vortex compared to SD initial states. However, this would result in weaker ARMs for lower initial-state decay rates, which is opposite to the trend observed in Figure 2a.

[41] Alternatively, the negative initial-state rate dependence may be a property of the MD component of PSD remanence. This would explain why it has the same sign as the MD effect but a smaller magnitude. If this is so, truly SD grains should have no initial-state effect, and the causes of the initial-state and the direct rate dependences of ARM intensity in the PSD range would be unrelated. The former would be an MD effect and the latter an SD effect.

7. Implications for Paleomagnetism and Paleointensity Determination

[42] The decay-rate dependence of ARM intensity poses a problem because ARM is frequently used as a standard for inter-laboratory calibration of instruments and because ARM is the most commonly used normalizing remanence in relative paleointensity studies. Samples in our study that had yielded reliable absolute (C6 C1) and relative (578 B) paleointensity results exhibited $\sim$7% variation in ARM intensity as the decay rate used in producing the ARM varied by an order of magnitude (Figure 1). How can we

correct for this potential source of error in comparing values of ARM obtained using different decay rates?

[43] In all samples tested, ARM differences disappeared after AF demagnetization to ∼0.3 of the initial intensity (Figure 3). Using $ARM_{0.3}$ rather than untreated ARM is a practical solution to the decay-rate problem. Note, however, that there is no single "best field" for AF treatment. $ARM_{0.3}$ is reached with AFs ranging from 10 mT (Figure 3b) to 40 mT (Figure 3a).

[44] Modern relative paleointensity studies do use partially demagnetized rather than untreated NRM and ARM. Optimum demagnetization is tuned to eliminating viscous overprints without rendering the signal unmeasurably weak. In recent studies, a wide variety of fields and temperatures were used: 10 mT [*Peck et al.*, 1996; *Yamazaki et al.*, 1995], 15 mT [*Verosub et al.*, 1996; *Yamazaki and Ioka*, 1994], 17.5 mT [*Tauxe and Hartl*, 1997], 20 mT [*Clement and Kent*, 1991; *Meynadier et al.*, 1994, 1995; *Tric et al.*, 1992; *Valet et al.*, 1994; *Yamazaki and Oda*, 2001, 2002], 25 mT [*Roberts et al.*, 1997], 30 mT [*Haag*, 2000; *Pan et al.*, 2001], 40 mT, [*Glen et al.*, 1999], averages of more than two steps [*Brachfeld and Banerjee*, 2000; *Channell et al.*, 2002; *Dinares-Turell et al.*, 2002; *Guyodo et al.*, 2001; *Meynadier et al.*, 1992], and thermal demagnetization to 420°C [*Laj et al.*, 1996].

[45] Since individual studies resulted in different fractions of initial ARM, there is a risk that records compiled from different studies [e.g., *Guyodo and Valet*, 1999] might be affected by the decay-rate dependence of ARM. Each study applies a single optimal demagnetization to an entire sedimentary sequence. Within such a study, any decay-rate dependence of ARM is probably unimportant because the whole unit was treated identically. However, more attention is called for in stacking results determined with different optimal demagnetizations and/or different instruments. The decay-rate dependence of ARM is unlikely to seriously distort major relative paleointensity trends since ARM intensity for PSD samples varies only a few% as the decay rate varies an order of magnitude (Figures 1 and 2). However, minor features might be enhanced in one record or suppressed in another by different demagnetization levels. For best stacking results, a common level of demagnetization in all records is advisable. To eliminate decay-rate effects, that level would be $ARM_{0.3}$.

8. Conclusions

[46] This study has both fundamental and practical implications. For truly SD grains, our study (0.065 μm magnetite) and that of *Egli and Lowrie* [2002] (tuff containing 0.016 μm magnetite) find that ARM intensities increase by 4–12% for an order of magnitude increase in AF exposure time (i.e., decrease in decay rate) during acquisition. Our approximate adaptation of *Néel*'s [1949] SD thermal activation theory and *Egli and Lowrie*'s [2002] exact treatment both predict increases of this order (Figure 4). PSD-size magnetites have the same experimental decay-rate dependence but the magnitude of the effect is smaller (Figure 1). This situation is the analog of the well-established SD/PSD cooling-rate dependence of TRM intensity.

[47] MD grains (16.9 μm magnetite, granites) have a wealth of previously unknown decay-rate properties. ARM decreases, rather than increasing, with increasing AF exposure time during acquisition, probably because the self-demagnetizing field has longer to act on loosely pinned domain walls. The same model explains the MD cooling-rate dependence of TRM [*Papusoi*, 1972b]. Tightly pinned walls show no acquisition decay-rate variation of their ARM, as demonstrated by unannealed grains (Figure 1) and by AF demagnetization following ARM production (Figure 3). However, tighter wall pinning in the initial demagnetized state (where the net self-demagnetizing field is zero) as a result of longer AF exposure is the probable cause of the initial-state decay-rate dependence, which has the opposite sign to the acquisition decay-rate response (Figure 2).

[48] These MD theoretical interpretations are speculative and there are no domain observations on MD magnetites in an ARM state to back them up, but they do account for all our results in a consistent way. They also explain the properties of PSD grains as a blend of SD and MD responses: SD-like but reduced acquisition decay-rate response (Figure 1), MD-like but reduced response to annealing (Figure 1), and MD-like initial-state decay-rate dependence (Figure 2).

[49] On the practical side, the dependence of ARM intensity on the AF decay rate used in producing it affects the ARM/susceptibility ratio, widely used as a grain size indicator, and the normalizing ARM intensity used in relative paleointensity determination to correct for differing magnetic mineral contents between samples. Because rate effects are small, errors in a set of measurements made in the same laboratory with a fixed decay rate are unlikely to be serious. However, inter-laboratory comparisons of standards and stacking of paleointensity records obtained in different laboratories would be on safer ground if $ARM_{0.3}$ (ARM demagnetized to 0.3 times initial intensity) were used instead of untreated ARM. The AF required to achieve $ARM_{0.3}$ varied in our work from 10 mT for small MD magnetite grains to 40 mT for SD grains, and must be tuned to the requirements of a particular study, including cleaning viscous and other secondary remanences as well as eliminating decay-rate differences.

[50] **Acknowledgments.** This research was supported by NSERC Canada grant A7709 to D.J.D. Stefanie Brachfeld generously donated a large collection of lake sediment samples for use in this study. We thank the referees for their careful reviews, which led to significant improvement of the paper.

References

Banerjee, S. K., J. King, and J. A. Marvin, A rapid method for magnetic granulometry with applications to environmental studies, *Geophys. Res. Lett.*, *8*, 333–336, 1981.

Biquand, D., Effet de la vitesse de refroidissement sur l'intensité de l'aimantation thermorémanente: Étude expérimentale, conséquences théoriques, *Can. J. Earth Sci.*, *31*, 1342–1352, 1994.

Brachfeld, S. A., and S. K. Banerjee, A new high-resolution geomagnetic relative paleointensity record for the North American Holocene: A comparison of sedimentary and absolute intensity data, *J. Geophys. Res.*, *105*, 821–834, 2000.

Channell, J. E. T., A. Mazaud, P. Sullivan, S. Turner, and M. E. Raymo, Geomagnetic excursions and paleointensities in the Matuyama chron at Ocean Drilling program Sites 983 and 984, *J. Geophys. Res.*, *107*(B6), doi:10.1029/2001JB000491, 2002.

Chauvin, A., Y. Garcia, P. Lanos, and F. Laubenheimer, Paleointensity of the geomagnetic field recovered on archaeomagnetic sites from France, *Phys. Earth Planet. Inter.*, *120*, 111–136, 2000.

Clement, B. M., and D. V. Kent, A southern hemisphere record of the Matuyama-Brunhes polarity reversal, *Geophys. Res. Lett.*, *18*, 81–84, 1991.

Dinares-Turell, J., L. Sagnotti, and A. P. Roberts, Relative geomagnetic paleointensity from the Jaramillo subchron to the Matuyama/Brunhes boundary as recorded in a Mediterranean piston core, *Earth Planet. Sci. Lett.*, *194*, 327–341, 2002.

Dodson, M. H., and E. McClelland-Brown, Magnetic blocking temperatures of single-domain grains during slow cooling, *J. Geophys. Res.*, *85*, 2625–2637, 1980.

Doh, S.-J., J. W. King, and M. Leinen, A rock magnetic study of giant piston core LL44-GPC3 from the central North Pacific and its paleoceanographic implications, *Paleoceanography*, *3*, 89–111, 1988.

Dunlop, D. J., Paleomagnetism of Archean rocks from northwestern Ontario, 4. Burchell Lake granite, Wawa-Shebandowan Subprovince, *Can. J. Earth Sci.*, *21*, 1098–1104, 1984.

Dunlop, D. J., Theory and application of the Day plot (M_{rs}/M_s versus H_{cr}/H_c), 1. Theoretical curves and tests using titanomagnetite data, *J. Geophys. Res.*, *107*(B3), 2056, doi:10.1029/2001JB000486, 2002.

Dunlop, D. J., and K. S. Argyle, Thermoremanence, anhysteretic remanence and susceptibility of submicron magnetites: Nonlinear field dependence and variation with grain size, *J. Geophys. Res.*, *102*, 20,199–20,210, 1997.

Dunlop, D. J., and Ö. Özdemir, *Rock Magnetism: Fundamentals and Frontiers*, 573 pp., Cambridge Univ. Press, New York, 1997.

Dunlop, D. J., and G. F. West, An experimental evaluation of single domain theories, *Rev. Geophys.*, *7*, 709–757, 1969.

Dunlop, D. J., L. D. Schutts, and C. J. Hale, Paleomagnetism of Archean rocks from northwestern Ontario, 3. Rock magnetism of the Shelley Lake granite, Quetico Subprovince, *Can. J. Earth Sci.*, *21*, 879–886, 1984.

Egli, R., and W. Lowrie, Anhysteretic remanent magnetization of fine magnetic particles, *J. Geophys. Res.*, *107*(B10), 2209, doi:10.1029/2001JB000671, 2002.

Fox, J. M. W., and M. J. Aitken, Cooling-rate dependence of thermoremanent magnetization, *Nature*, *283*, 462–463, 1980.

Glen, J. M. G., J. C. Liddicoat, and R. S. Coe, A detailed record of paleomagnetic field change from Searles Lake, California 1. Long-term secular variation bounding the Gauss/Matuyama polarity reversal, *J. Geophys. Res.*, *104*, 12,865–12,882, 1999.

Guyodo, Y., and J.-P. Valet, Global changes in intensity of the Earth's magnetic field during the past 800 kyr, *Nature*, *399*, 249–252, 1999.

Guyodo, Y., G. D. Acton, S. Brachfeld, and J. E. T. Channell, A sedimentary paleomagnetic record of the Matuyama chron from the Western Antarctica margin (ODP site 1101), *Earth Planet. Sci. Lett.*, *191*, 61–74, 2001.

Haag, M., Reliability of relative paleointensities of a sediment core with climatically-triggered strong magnetization changes, *Earth Planet. Sci. Lett.*, *180*, 49–59, 2000.

Halgedahl, S. L., R. Day, and M. Fuller, The effect of cooling rate on the intensity of weak-field TRM in single-domain magnetite, *J. Geophys. Res.*, *85*, 2698–3690, 1980.

Johnson, H. P., W. Lowrie, and D. V. Kent, Stability of anhysteretic remanent magnetization in fine and coarse magnetite and maghemite particles, *Geophys. J. R. Astron. Soc.*, *41*, 1–10, 1975.

King, J. W., S. K. Banerjee, and J. Marvin, A new rock magnetic approach to selecting sediments for geomagnetic paleointensity studies: Application to paleointensity for the last 4000 years, *J. Geophys. Res.*, *88*, 5911–5921, 1983.

Laj, C., C. Kissel, and I. Lefevre, Relative geomagnetic field intensity and reversals from upper Miocene sections in Crete, *Earth Planet. Sci. Lett.*, *141*, 67–78, 1996.

Levi, S., and S. K. Banerjee, On the possibility of obtaining relative paleointensities from lake sediments, *Earth Planet. Sci. Lett.*, *29*, 219–226, 1976.

Levi, S., and R. T. Merrill, A comparison of ARM and TRM in magnetite, *Earth Planet. Sci. Lett.*, *32*, 171–184, 1976.

Lowrie, W., and M. Fuller, On the alternating field demagnetization characteristics of multidomain thermoremanent magnetization in magnetite, *J. Geophys. Res.*, *76*, 6339–6449, 1971.

McClelland-Brown, E., Experiments on TRM intensity dependence on cooling rate, *Geophys. Res. Lett.*, *11*, 205–208, 1984.

McNab, T. K., R. A. Fox, and J. F. Boyle, Some magnetic properties of magnetite (Fe_3O_4) microcrystals, *J. Appl. Phys.*, *39*, 5703–5711, 1968.

Meynadier, L., J.-P. Valet, R. Weeks, N. J. Shackleton, and V. L. Hagee, Relative geomagnetic intensity of the field during the last 140 ka, *Earth Planet. Sci. Lett.*, *114*, 39–57, 1992.

Meynadier, L., J.-P. Valet, F. C. Bassinot, N. J. Shackleton, and Y. Guyodo, Asymmetrical saw-tooth pattern of the geomagnetic field intensity from equatorial sediments in the Pacific and Indian Oceans, *Earth Planet. Sci. Lett.*, *126*, 109–127, 1994.

Meynadier, L., J.-P. Valet, and N. J. Shackleton, Relative geomagnetic intensity during the last 4 million years from the equatorial Pacific, *Proc. Ocean Drill. Program Sci. Res.*, *138*, 779–795, 1995.

Moskowitz, B. M., R. B. Frankel, S. A. Walton, D. P. E. Dickson, K. K. W. Wong, T. Douglas, and S. Mann, Determination of the pre-exponential frequency factor for superparamagnetic maghemite particles in magnetoferritin, *J. Geophys. Res.*, *102*, 22,671–22,680, 1997.

Néel, L., Théorie du traînage magnétique des ferromagnétiques en grains fins avec applications aux terres cuites, *Ann. Géophys.*, *5*, 99–136, 1949.

Néel, L., Some theoretical aspects of rock magnetism, *Adv. Phys.*, *4*, 191–243, 1955.

Pan, Y., R. Zhu, J. Shaw, Q. Liu, and B. Guo, Can relative paleointensities be determined from the normalized magnetization of the wind-blown loess of China?, *J. Geophys. Res.*, *106*, 19,221–19,232, 2001.

Papusoi, C., Effet de la vitesse de refroidissement sur l'intensité de l'aimantation thermorémanente d'un ensemble de grains monodomaines, *Ann. Univ. Al. I. Cuza Iasi, Sect. 1b Phys.*, *18*(1), 31–47, 1972a.

Papusoi, C., Variation de l'intensité de l'aimantation thermorémanente d'un ensemble de grains à structure de polydomaines magnétiques en fonction de la vitesse de refoidissement, *Ann. Univ. Al. I. Cuza Iasi, Sect. 1b Phys.*, *18*(2), 155–166, 1972b.

Peck, J. A., J. W. King, S. M. Colman, and V. A. Kravchinsky, An 84-kyr paleomagnetic record from the sediments of Lake Baikal, Siberia, *J. Geophys. Res.*, *101*, 11,365–11,385, 1996.

Perrin, M., Paleointensity determination, magnetic domain structure, and selection criteria, *J. Geophys. Res.*, *103*, 30,591–30,600, 1998.

Pullaiah, G., E. Irving, K. L. Buchan, and D. J. Dunlop, Magnetization changes caused by burial and uplift, *Earth Planet. Sci. Lett.*, *28*, 133–145, 1975.

Roberts, A. P., B. Lehman, R. J. Weeks, K. L. Verosub, and C. Laj, Relative paleointensity of the geomagnetic field over the last 200,000 years from ODP sites 883 and 884, North pacific Ocean, *Earth Planet. Sci. Lett.*, *152*, 11–23, 1997.

Shcherbakova, V. V., V. P. Shcherbakov, and F. Heider, Properties of partial thermoremanent magnetization in pseudosingle domain and multidomain magnetite grains, *J. Geophys. Res.*, *105*, 767–781, 2000.

Stacey, F. D., and S. K. Banerjee, *The Physical Principles of Rock Magnetism*, 195 pp., Elsevier Sci., New York, 1974.

Stoner, J. S., J. E. T. Channell, and C. Hillaire-Marcel, Magnetic properties of deep-sea sediments off southwest Greenland: Evidence for major differences between the last two deglaciations, *Geology*, *23*, 241–244, 1995.

Sugiura, N., ARM, TRM and magnetic interactions: Concentration dependence, *Earth Planet. Sci. Lett.*, *46*, 438–442, 1979.

Tauxe, L., Sedimentary records of relative paleointensity of the geomagnetic field: Theory and practice, *Rev. Geophys.*, *31*, 319–354, 1993.

Tauxe, L., and P. Hartl, 11 million years of Oligocene geomagnetic field behavior, *Geophys. J. Int.*, *128*, 217–229, 1997.

Tauxe, L., T. Pick, and Y. S. Kok, Relative paleointensity in sediments: A pseudo-Thellier approach, *Geophys. Res. Lett.*, *22*, 2885–2888, 1995.

Tric, E., J.-P. Valet, P. Tucholka, M. Paterne, L. Labeyrie, F. Guichard, L. Tauxe, and M. Fontugne, Paleointensity of the geomagnetic field during the last 80,000 years, *J. Geophys. Res.*, *97*, 9337–9351, 1992.

Valet, J.-P., L. Meynadier, F. C. Bassinot, and F. Garnier, Relative paleointensity across the last geomagnetic reversal from sediments of the Atlantic, Indian and Pacific Oceans, *Geophys. Res. Lett.*, *21*, 485–488, 1994.

Verosub, K. L., and A. P. Roberts, Environmental magnetism: Past, present, and future, *J. Geophys. Res.*, *100*, 2175–2192, 1995.

Verosub, K. L., E. Herrero-Bervera, and A. P. Roberts, Relative geomagnetic paleointensity across the Jaramillo subchron and the Matuyama/Brunhes boundary, *Geophys. Res. Lett.*, *23*, 467–470, 1996.

Walton, D., Time-temperature relations in the magnetization of assemblies of single-domain grains, *Nature*, *286*, 245–247, 1980.

Walton, D., and W. Williams, Cooling rate effects in the magnetization of single-domain grains, *J. Geomagn. Geoelectr.*, *40*, 727–729, 1988.

Yamazaki, T., and N. Ioka, Long-term secular variation of the geomagnetic field during the last 200 kyr recorded in sediment cores from the western equatorial Pacific, *Earth Planet. Sci. Lett.*, *128*, 527–544, 1994.

Yamazaki, T., and N. Ioka, Cautionary note on magnetic grain-size estimation using the ratio of ARM to magnetic susceptibility, *Geophys. Res. Lett.*, *24*, 751–754, 1997.

Yamazaki, T., and H. Oda, A Brunhes-Matuyama polarity transition record from anoxic sediments in the South Atlantic (Ocean Drilling Program Hole 1082C), *Earth Planets Space*, *53*, 817–827, 2001.

Yamazaki, T., and H. Oda, Orbital influence on Earth's magnetic field: 100,000 year periodicity in inclination, *Science*, *295*, 2435–2438, 2002.

Yamazaki, T., N. Ioka, and N. Eguchi, Relative paleointensity of the geomagnetic field during the Brunhes chron, *Earth Planet Sci. Lett.*, *136*, 525–540, 1995.

Yang, S., J. Shaw, and Q. Y. Wei, Tracking a non-dipole geomagnetic anomaly using new archeointensity results from north-east China, *Geophys. J. Int.*, *115*, 1189–1196, 1993.

York, D., Magnetic blocking temperature, *Earth Planet. Sci. Lett.*, *39*, 94–97, 1978.
Yu, Y., Rock magnetic and paleomagnetic experiments on hemoilmenites and titanomagnetites in some volcanic rocks from Japan, M.S. thesis, 24 pp., Univ. of Toronto, Mississauga, Ontario, 1998.
Yu, Y., and D. J. Dunlop, Paleointensity determination on the late Precambrian Tudor Gabbro, Ontario, *J. Geophys. Res.*, *106*, 26,331–26,343, 2001.
Yu, Y., and D. J. Dunlop, Multivectorial paleointensity determination from the Cordova Gabbro, southern Ontario, *Earth Planet. Sci. Lett.*, *203*, 983–998, 2002.
Yu, Y., D. J. Dunlop, and Ö. Özdemir, Properties of partial anhysteretic remanent magnetization in magnetite, 1. Additivity, *J. Geophys. Res.*, *107*(B10), 2244, doi:10.1029/2001JB001249, 2002.
Yu, Y., D. J. Dunlop, and Ö. Özdemir, Are ARM and TRM analogs?, Thellier analysis of ARM and pseudo-Thellier analysis of TRM, *Earth Planet. Sci. Lett.*, *205*, 325–336, 2003.

D. J. Dunlop and Y. Yu, Geophysics, Department of Physics, University of Toronto, 3359 Mississauga Road North, Mississauga, Ontario, Canada L5L 1C6. (yjyu@physics.utoronto.ca; dunlop@physics.utoronto.ca)